Anomalous Protonic-Glass Evolution from Ordered Phase in NH···N Hydrogen-Bonded DabcoHBF$_4$ Ferroelectric

Armand Budzianowski and Andrzej Katrusiak*

Faculty of Chemistry, Adam Mickiewicz University, Grunwaldzka 6, 60-780 Poznań, Poland

Marek Szafrański*

Faculty of Physics, Adam Mickiewicz University, Umultowska 85, 61-614 Poznań, Poland

Received: February 14, 2008; Revised Manuscript Received: September 23, 2008

Dielectric properties, spontaneous polarization, and phase transitions of the NH$^+$···N bonded ferroelectric dabcoHBF$_4$ (i.e., 1,4-diazabicyclo[2.2.2]octane tetrafluoroborate, $[C_6H_{13}N_2]^+ \cdot BF_4^-$) have been related to one-dimensional arrangement of the cations and to their conformational properties. The onset of conformational transformation lowering the symmetry of the cations, rearrangement of the anions, and proton disordering in NH$^+$···N hydrogen bonds, linking the cations into linear chains, lead to a ferroelectric−ferroelectric phase transition at $T_{23} = 153$ K. A weak coupling between the protonic and anionic sites in dabcoHBF$_4$ results in the formation of distinct phase-diagram regions: the high-temperature paraelectric phase with disordered protons, the intermediate ferroelectric phase with the protons ordered, and the low-temperature ferroelectric phase where the protons become disordered again. The lowest temperature phase remains ferroelectric owing to the ionic displacements, while the protons assume the glass state. In this phase the H$^+$ transfers involve local formation of neutral, monocationic, and dicationic species. Such an anomalous formation of protonic glass state from the ordered phase depends on the subtle structural features pertaining to the proton transfers in bistable hydrogen bonds. In paraelectric phase I, between the mp and $T_{12} = 374$ K, the anions are orientationally disordered, the protons are disordered in the hydrogen bonds and the cations rotate about the [*z*] direction; in ferroelectric phase II below T_{12}, the protons and cations order, the dabco cations assume a planar conformation of ethylene bridges, and the anions exhibit a residual temperature-dependent gradual ordering (two 80:20 occupied sites of the anion are still observed at 332 K); and in ferroelectric phase III below T_{23}, the cations assume left- and right-twisted propeller conformations and the anions are ordered but the protons become disordered in the hydrogen bonds.

I. Introduction

Recently described NH$^+$···N hydrogen-bonded ferroelectrics[1,2] are in certain respects similar and in others considerably different than their OH···O bonded counterparts. The latter group, often referred to as KDP-type ferroelectrics (KDP denotes prototypic KH_2PO_4), belongs to the most intensively studied crystal structures because it was regarded as a simple illustration of properties of hydrogen bonds in crystals in relation to phase transitions and also of dynamical transformations of H-bonds in biological systems.[3,4] It is characteristic of the KDP-type ferroelectrics that above T_c the H-atoms in the OH···O hydrogen bonds become dynamically disordered. Another feature of the KDP-type ferroelectrics is the negative $\partial T_c/\partial p$, connected with the decreased O···O distance, lowered energy-barrier between the proton sites, and decreased distortions of molecules or ions from prototypical symmetry of the crystal.[5] For the NH$^+$···N bonded ferroelectrics a positive $\partial T_c/\partial p$ has been observed.[6]

In the present study, we have examined the coupling between the ionic arrangements and the protonic sites, by investigating the low-temperature phase transition between two ferroelectric phases of dabcoHBF$_4$.[7,8] Its structure can transform in several ways and the contribution of particular factors to the thermodynamic stability of the ferroelectric phases is disputable. It was postulated, that transformations of dabco compounds could be induced by conformational properties of the dabco cation, which at high temperature has its three ethylene bridges aligned (i.e., the N−C−C−N torsion angles equal to 0°) and at low temperatures twisted (to about 15°). Such a conformational transformation breaks the molecular and crystal mirror-plane symmetry. However the dabcoHBF$_4$ structure can also transform in other ways. The proton can change its site in the NH$^+$···N hydrogen bonds, the cations and anions can change their orientations, and shift one with respect to their neighbors. These structural features are quite common for hydrogen-bonded crystals. Meanwhile, the recent study of the phase transitions in analogous ferroelectric dabcoHClO$_4$ revealed no changes in the conformation of the cations.[9]

The space-group symmetry *P*4/*mmm* of the paraelectric phase I of dabcoHBF$_4$ above $T_{12} = 374$ K, and space group $Pm2_1n$ of the ferroelectric phase II below T_{12} were determined previously.[1,9–11] In this paper, we describe the crystal structure of a new ferroelectric phase III of dabcoHBF$_4$, transforming from phase II on cooling below $T_{23} = 153$ K. For the ferroelectric phases II and III we report the relations between the ferroelectric properties of dabcoHBF$_4$ and its crystal structure, the chemical and conformational transformations of the dabco molecules and ions, and specific features of the dabcoHBF$_4$ crystal related to the high polarizability of the NH$^+$···N hydrogen bonds.[12,13] The systematic description of the structure and polarizability of

* To whom correspondence should be addressed. E-mails: A.K., katran@amu.edu.pl; M.S., masza@amu.edu.pl.

10.1021/jp801316a CCC: $40.75 © 2008 American Chemical Society
Published on Web 11/19/2008

$NH^+\cdots N$ bonds becomes crucial in the view of the recent studies on the unusual dielectric properties of the pyrazine and dabco H-bonded complexes.[14,15] It is shown below that the protons behavior in the $NH^+\cdots N$ bonds of dabcoHBF$_4$ in its low-temperature ferroelectric phase is drastically different than in most substances with bistable hydrogen bonds, and specifically from that in $OH^+\cdots O$ bonded KDP-type ferroelectrics.

II. Experimental Details

The samples for single-crystal experiments were slowly crystallized from aqueous solution. Then they were carefully selected and gently glued to glass fibers, to avoid strains in these susceptible samples. To minimize the effects of the strains generated at phase transitions, the crystal quality was carefully checked and several samples had to be used. X-ray diffraction analysis was carried out using KUMA diffractometers, one equipped with a single-point detector was used for measuring unit-cell parameters between 93.6 and 420 K and intensities at selected temperature points, and the second one with a charge-coupled device (CCD) camera for data collection. Temperature was calibrated within 1 K, and the relative changes within 0.1 K. The data were processed routinely and the structure of phase III was solved by direct methods.[16] All structures of phase III were refined with anisotropic thermal parameters by full-matrix least-squares.[17] All H atoms (including the disordered proton) were located from difference-Fourier maps and refined with isotropic thermal parameters at all temperatures in phase III, except for the measurement at 150.6 K close to T_{23}, where all H atoms were placed in geometrically ideal positions after each cycle of the refinements; where the U_{iso} of the H-atoms departed from expected magnitudes, they were calculated as 1.2 of U_{eq} of their carriers. The location of the proton and its anomalous behavior in the function of temperature was checked in several ways, for example by reducing the crystal symmetry or assigning the protons to specific N atoms. The low temperature diffractometric determinations were repeated many times for differently grown crystals and by applying different criteria for choosing the samples, as well as for varied cooling speeds of the crystal through the transition point at $T_{23} = 153$ K. Also the samples were annealed for several days at the temperature immediately below T_{23}. A special care was taken to record the history of investigated samples. The intensity data collections included all symmetry-dependent reflections (full sphere of data), and rigorous symmetry tests were carried out for the phase III; several hypothetical, lowered-symmetry space groups of the crystal, were tested (e.g., $P2_1$, $P1$), however in all these cases the disordered proton appeared in two sites. Finally the model with disordered protons for which the best R factors were obtained, was accepted (see Figure 1). In phase II close to T_{23}, the structure was refined with all the C, N, B, and F atoms anisotropic and the H-atoms isotropic. At 332 K, a partial disordering of the BF_4 anion in two sites and orientations has been observed. At 332 K, the BF_4 anion is disordered in this way that two B sites are 0.64(2) Å apart, and one of the B−F bonds is directed up the [z] axis and another B−F bonds down this axis. The occupation of these two sites refined to 0.804:0.196(7). In this model the atoms at less-occupied sites were refined with U_{iso} parameters only. At 370 K the best convergence was obtained for the B1 atom in one central site, and the F atoms disordered in several orientations about it (five F sites at 370 K and six F sites at 375 K). Attempts to refine more F sites assigned to difference Fourier peaks appearing at about 1.4 Å about the B1 atom did not significantly improve the results. In the final models above 330 K all atoms were isotropic,

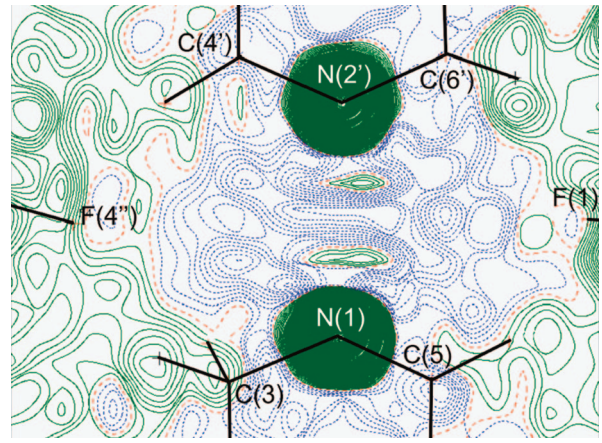

Figure 1. Fourier-map section through the $NH^+\cdots N$ hydrogen bond of the dabcoHBF$_4$ structure at 93.6 K, showing the peaks corresponding to the proton disordered at N(1) and N(2). The contours indicate the 0.002 e Å^{-3} levels, and the dashed contours outline the negative density regions (due to the Fourier-series termination errors). The projections of other atoms onto the section plane have been also shown for clarity; the primes denote atoms at x, y, $z + 1$.

TABLE 1: Selected Crystal Data of DabcoHBF$_4$ in the Paraelectric Phase I (above 378 K) and in Two Ferroelectric Phases II (378−154.5 K) and III (below 153 K)

	phase I	phase II	phase III
T (K)	405	224.3	119.2
space group	*P4/mmm*	*Pm*2$_1$*n*	*Pb*2$_1$a
a (Å)	6.589(3)	8.560(1)	16.694(5)
b (Å)	6.589(3)	9.644(1)	9.699(2)
c (Å)	5.357(2)	5.330(1)	5.318(2)
V (Å^3)	232.6(5)	440.0(1)	861.1(5)
Z	1	2	4
D_x (g/cm^3)	1.427	1.509	1.543

and the ethylene H-atoms and the proton were located from the molecular geometry, with their U_{iso} 1.2 larger that that of their carriers.

Selected crystal data representative for phases I, II, and III are listed in Table 1. The atomic coordinates for these structures and the full documentation for all structural determinations at 11 temperatures have been deposited in the Cambridge Crystallographic Data Center as 15 supplementary publications Nos. CCDC 676638−676652. Copies are included in the Supporting Information and may be also obtained free of charge on request from www.ccdc.cam.ac.uk.

The complex electric permittivity of dabcoHBF$_4$ was measured along the ferroelectric b-axis (perpendicular to the $NH^+\cdots N$ bonded chains) and along the c-axis (parallel to the $NH^+\cdots N$ bonded chains) of the ferroelectric phase II, with a Hewlett-Packard 4192A impedance analyzer. The specimens were prepared in the form of thin plates with silver-painted electrodes. The temperature was changed continuously with a rate of 0.5 K/min. The spontaneous polarization was measured in the temperature range from 100 to 390 K by pyroelectric method using an electrometer type W7-30. The single-domain crystals with silver electrodes deposited on the surfaces perpendicular to the ferroelectric axis of the crystal were heated with a rate of 2 K/min.

III. Results and Discussion

The present detailed X-ray diffraction study of the phase transition at T_{23} between two ferroelectric phases of dabcoHBF$_4$ allows the dielectric properties of this crystal to be related to its

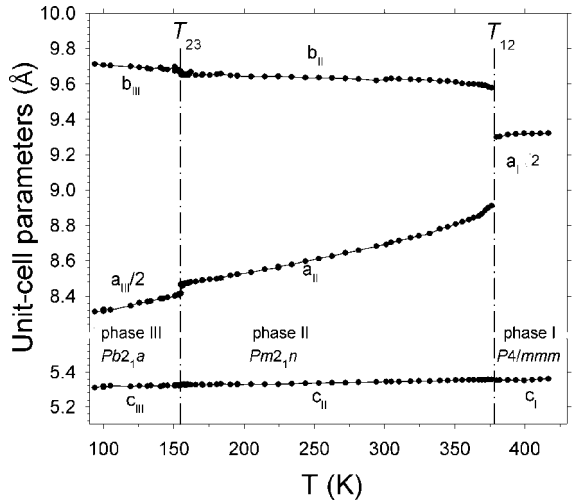

Figure 2. Temperature dependence of the unit-cell dimensions of dabcoHBF$_4$. The length of diagonal $[110]_I$ of the tetragonal unit-cell, and half of parameter a_{III} in phase III, have been given for convenient comparisons with the corresponding dimensions of the lattice of room-temperature phase II.

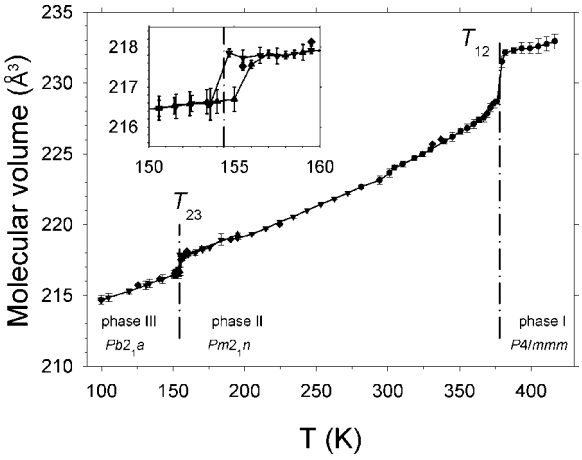

Figure 3. Temperature dependence of the unit-cell volume per one dabcoHBF$_4$ formula unit in the crystalline state. The inset shows the details of the T_{23} region, with the thin lines tracing the measurement points of the heating and cooling runs (indicated by arrows). The lines joining the points have been drawn for guiding the eyes only.

structure. The structural transformations can be described in terms of: (i) ionic displacements; (ii) conformational changes of the cation; and (iii) proton transfers between the donor and acceptor sites in the NH$^+$···N bonds leading to charge defects and short-range polar regions.[18,19] The coupling between these effects, their contribution to the crystal spontaneous polarization and dielectric response of the crystal, and the origin of the protonic-glass state in the low-temperature phase III are discussed below.

A. Thermal Expansion. The thermal expansion about the ferroelectric−ferroelectric phase transition in dabcoHBF$_4$ at T_{23} has several specific features. The unit-cell dimensions (Figures 2 and 3) change only slightly except for parameter a, which doubles below T_{23}. All unit-cell translations a, b, and c exhibit discontinuities at T_{23} testifying to the first-order character of the phase transition, which is most clearly seen for translation a and for the molecular volume. The noncontinuous character of the phase transition is apparent from the temperature dependence of reflections intensities, illustrated for several selected reflections in Figure 4. Moreover, the volume jump of ca. 1 Å^3 proceeds with a clear hysteresis of few tenth of a degree observed by the diffractometric measurements (see the inset in Figure 3).

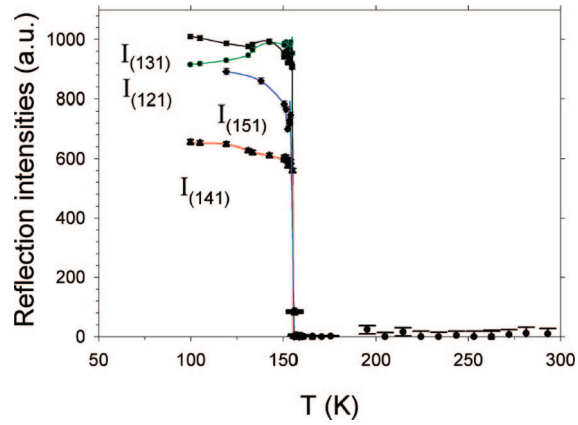

Figure 4. Temperature dependence of measured intensities of four selected reflections (their Miller indices shown as subscripts in parentheses), which should disappear when the dabcoHBF$_4$ crystal transforms from phase III to phase II.

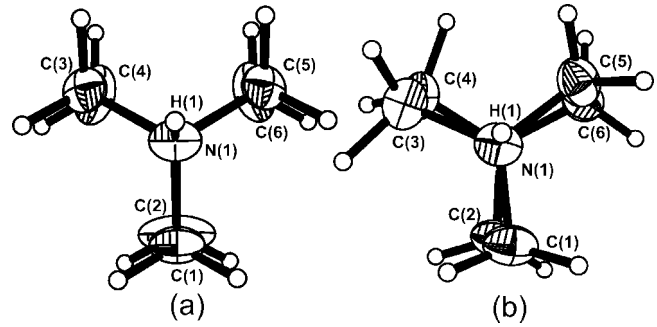

Figure 5. DabcoHBF$_4$ cation projected along the N(1)···N(2) direction [atom N(2) lies under N(1)]: (a) nontwisted conformation at 156 K in phase II and (b) propeller conformation at 134 K in phase III. The thermal ellipsoids have been drawn at the 50% probability level.

B. Conformation of the Cation. A characteristic feature of dabco salts is a possibility of conformational transformations of the cations.[18] In dabcoHBF$_4$ at room temperature the ethylene bridges $-CH_2-CH_2-$ and two N atoms are coplanar: one ethylene is located on a mirror plane and the other two are mutually related by the mirror plane and lie in a general position, but their torsion angle is of 0° within error. At T_{23} an onset of torsional twisting of the NCH_2CH_2N bonds results in the propeller-like conformation of the cation, illustrated in Figure 5. This breaks the mirror-plane symmetry of the cation, and of the crystal. The magnitude of this conformational transformation can be measured by the torsional angles N−C−C−N along the ethylene bridges. As shown in Figure 6, immediately below T_{23} the magnitudes of all these torsion angles change abruptly, and at still lower temperatures they slowly converge—two of them to about 16° and one to over 18°. The temperature dependence of the torsion angles is consistent with the noncontinuous character of the phase transition.

It is characteristic that with lowering temperature in phase II the intramolecular N···N distance monotonically increases and a pronounced elongation of this distance occurs below T_{23} (Figure 7). A very similar in shape, but reciprocal, is the temperature dependence of the intermolecular N···N distance of the hydrogen bond.

It has been also observed in the structural models between T_{23} and 223.3 K that the thermal ellipsoids of the carbon atoms bonded to nonprotonated N2 are considerably longer perpendicular to their bonds than those of the carbons bonded to the protonated N1 (see Figure 5). This systematically increased

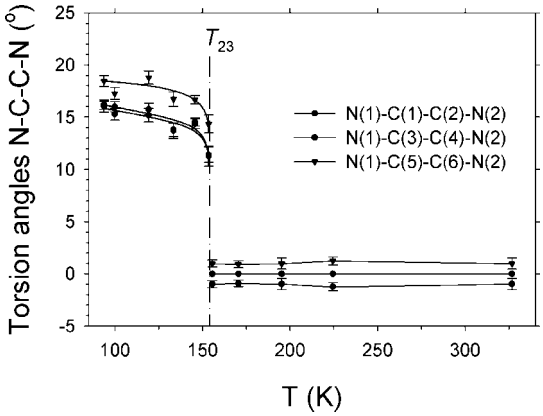

Figure 6. Temperature dependence of the ethylene torsion angles N−C−C−N in the dabcoHBF$_4$ cation.

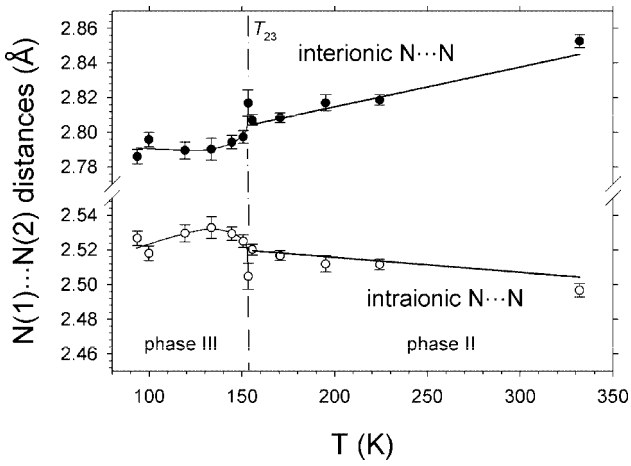

Figure 7. Temperature dependence of the N···N distances within the dabcoHBF$_4$ cation (open circles) and between the H-bonded cations (full circles). The lines have been fitted to these N···N distances separately in phases II and III.

amplitudes of the atomic displacements can be connected with the possible conformations of the cation: the left and right propeller and the metastable planar one. It is characteristic that the interionic distances of atoms C1 and C3, these with smaller displacement ellipsoids, are shorter than those of atoms C2 and C4: at 155.5 K C1···F3′ (symmetry code: x, y, $z + 1$) is 3.325 Å; C2···F3 is 3.473 Å; C3···F2″ (symmetry code: $0.5 - x$, $0.5 + y$, $1 - z$) is 3.271 Å; and C4···F2‴ (symmetry code: x, $y + 1$, z) is 3.378 Å. In this respect the surrounding about the carbon atoms bonded to N1 is tighter than that about the carbons bonded to N2, and these letter carbons are freer to vibrate stronger. These vibrations are likely to be anharmonic and associated with transitions between the left and right propeller and planar conformations. This interpretation of the displacement ellipsoids is consistent with the results of calorimetric measurements. As has been shown, the model of 3-fold conformational cationic disorder in phase II and the experimentally observed two conformational states of the cation in phase III, give a satisfactory explanation of the transition entropy gain at T_{23}.[8]

C. Crystal Symmetry and Structure. Below T_{23} the conformation of all cations in one chain is twisted in one sense about the N···N axis (compare Figures 8 and 9). It breaks the site symmetry of the cations and the crystal mirror-plane perpendicular to [100]. The largest structural rearrangement, when the magnitudes of atomic displacements are concerned, is that of the anions. In phase II, the anions are oriented in this way that one of the B−F bonds is aligned either nearly parallel

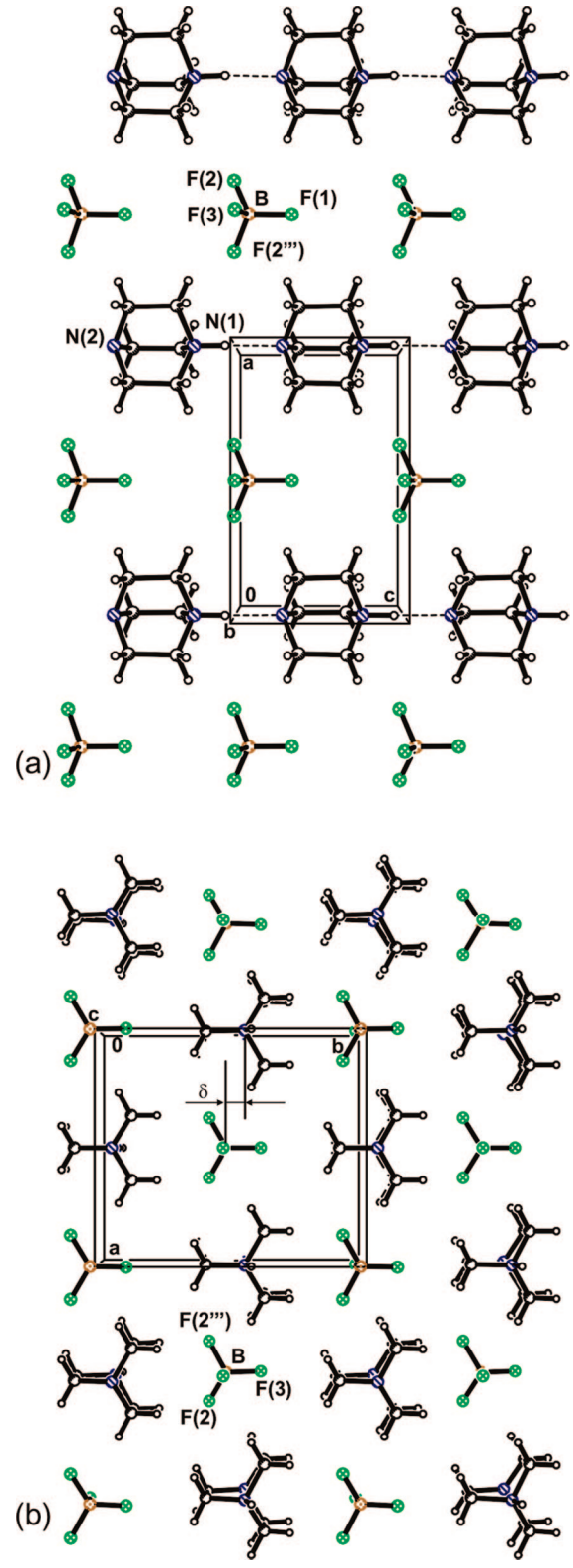

Figure 8. Autostereograms of the phase II structure at 162 K, viewed along crystal direction [010] (a) and [001] (b). The ionic displacement δ between the centers of the cation and the anion along [y], generating the spontaneous polarization of this crystal, has been indicated with arrows in drawing (b).

or antiparallel to the [001] direction, as illustrated in Figure 8, and sheets of anions with the B−F bonds parallel to [001] and these antiparallel to [001] are arranged consecutively perpendicular to [100]. In phase III (Figure 9), the anions rearrange into double sheets: two neighboring sheets perpendicular to

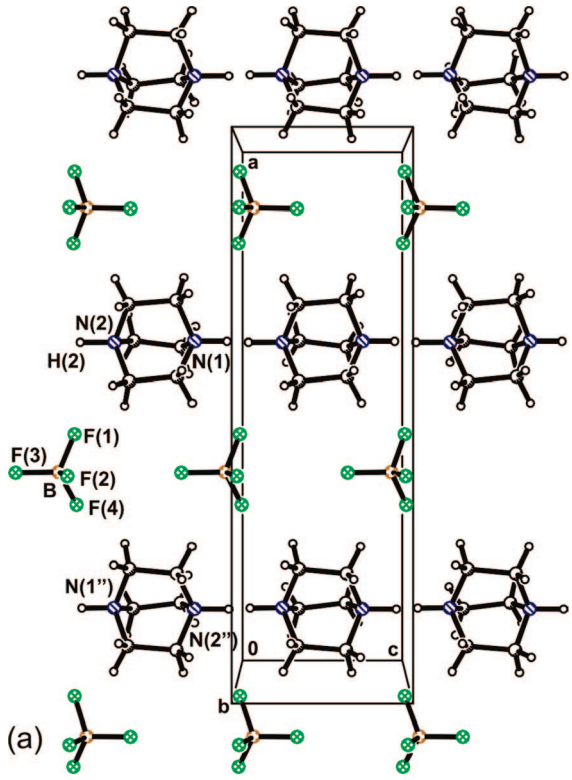

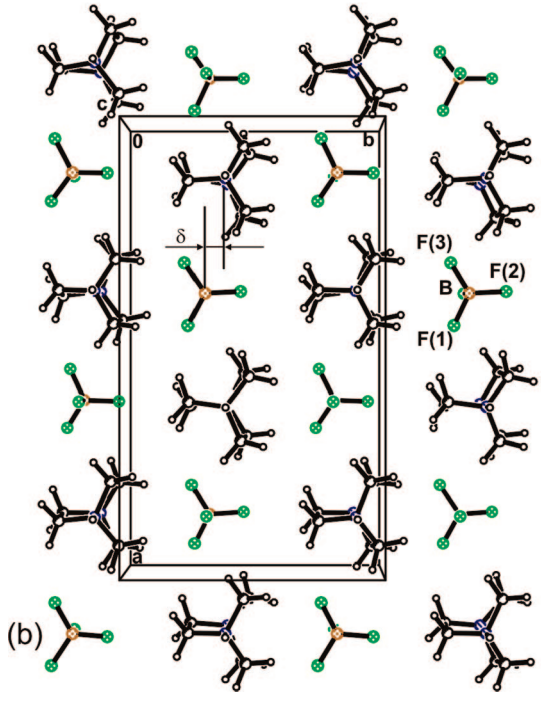

Figure 9. Autostereogram of low-temperature phase III crystal structure at 150.6 K viewed along (a) the [010] axis and (b) [001]. Two half-occupied sites for each proton have been indicated (see the text). The primed labels denote atoms transformed by the mirror plane perpendicular to *a*.

[100] comprise of anions with one B−F bond parallel to [001] and in two next sheets perpendicular to [100] the B−F bonds are antiparallel to [001]. This rearrangement of the anions together with the differentiation of cations conformation lower the crystal symmetry in phase III and lead to the doubling of the unit-cell translation along [100]. In phase III, the cations in

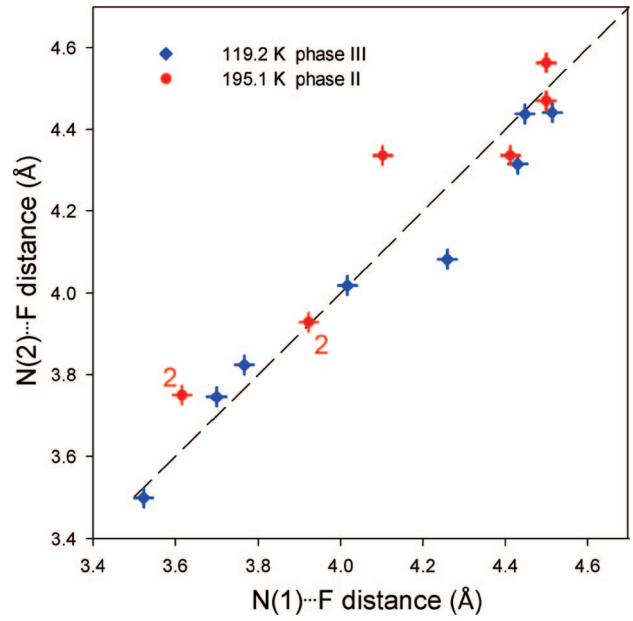

Figure 10. Distance−distance plot for the N···F contacts shorter than 5.0 Å at 195.1 K in phase II (red circles) and at 119.2 K in phase III (blue diamonds). The splitting of degenerated (overlaid) distances in phase II, when the symmetry lowers in phase III, is indicated by the degeneration number (2 twice); the dashed line marks the equidistant positions in the plot.

two neighboring sheets of chains (perpendicular to [100]) acquire a right-handed propeller conformation, and the cations in consecutive two next sheets, the left-handed propeller conformation. The structure transformation between phases II and III, and in particular the reorientations of the BF_4^- anions, have also considerable consequences for the proton site in the hydrogen bonds.

D. Proton Transfer. According to the symmetry requirements of phase III, the polarization of the chains should also change in this way that all the chains of the cations in the right-handed propeller conformation be polarized antiparallel to the chains of the left-handed cations. Thus if in phase III the protons were ordered at N(2), in the right-handed cations in Figure 9b they would point toward the reader, and the protons of the left-handed cations would point downward. Such a hypothetical structure with ordered protons would require, that on transformation from phase II to phase III at T_{23} the protons change their sites in this manner that in all the chains within two layers perpendicular to [100] the protons are not transferred, in the next two layers the protonic sites are changed, in the next two layers the protons are not transferred, and so on (compare Figures 8 and 9). Meanwhile, the structural results for phase III in temperature below T_{23} show, that the protons become disordered with equal occupancy in two sites at N(1) and at N(2). At the same time it is apparent from the dielectric response of dabcoHBF$_4$ and its very high polarizability, that the protons can relatively freely change their sites in phase III. This result is consistent with the shortening of the interionic distance N···N below T_{23}. It is also consistent with the rearrangement of the anions around the hydrogen bond. It appears from the interatomic distances plotted in Figure 10, that the electrostatic potential of the close anions more strongly stabilize the protonic site at N(1) in phase II, whereas in the structure of phase III the nearest fluorine and boron atoms are practically equidistant to atoms N(1) and N(2).

Thus one of possible reasons for proton disordering in phase III is the absence of electrostatic interactions, which would favor

one of the H^+ sites. As can be seen in Figure 10, in phase II where the protons are ordered, all shortest contacts of F atoms in the 4.4 Å range are closer to N(1) than to N(2). When symmetry lowers in phase III, of six F···N distances in this 4.4 Å range, three are slightly shorter for N(1) and the other two (including the shortest one) are shorter for N(2). Thus the electrostatic attraction to electronegative F atoms of the anions favors neither of the proton sites in phase III.

In all diffraction studies of phase III (see Experimental Details) the proton is disordered in two sites: one of them at about 1 Å from atom N(1) and the other site at about 1 Å from atom N(2). (Figure 1). Therefore it has been concluded that proton H(1) is randomly disordered in phase III. The disordered location of proton H(1) in phase III may result from a week coupling of its position with other structural transformations taking place below T_{23}, from the low potential-energy barrier separating the minima of the two-well function describing the H(1) proton position,[8,13] and also from the specific properties of the dabco molecules which can exist in the neutral, monocationic and dicationic forms. The symmetry change between phases II and III requires, that the protons transfer to the opposite N-atoms in the hydrogen bonds in every second chain along [100]. This can be clearly observed by comparing Figures 8a and 9a, where both sites of the disordered H(1) atom are shown in Figure 9a of phase III. The structural transformations accompanying the symmetry change also affect the orientation of the T_4-symmetric BF_4 anions. Thus in phase II in the layer shown in Figure 8a all anions have the same orientation, while in phase III the columns of anions assume an antiparallel orientation along [001] (Figure 9a).

Due to the specific features of the NH^+···N hydrogen bonds listed above, a very low disproportionation energy between neutral, monocationic and dicationic forms, and due to the absence of significant factors which would couple the protonic positions along isolated NH^+···N bonded chains, the correlation of the proton positions along the chains is very small.[19,20] Consequently it is plausible that the correlation length along [001] is short, which is a likely cause of the disorder of protons observed in phase III. The formation of such short-range polar regions in phase III of dabcoHBF$_4$, as inferred from the structural results and dielectric measurements (see below), is consistent with the observed polar arrangement of the NH^+···N bonded chains in the analogous dabcoHReO$_4$ ferroelectric.[2]

E. Spontaneous Polarization. Temperature dependence of spontaneous polarization $P_s(T)$ measured for a high-quality single-domain dabcoHBF$_4$ crystal is shown in Figure 11. The polarization of the crystal vanishes suddenly at $T_{12} = 378$ K, which is consistent with a first-order character of the ferroelectric-paraelectric phase transition. The temperature dependence of P_s qualitatively resembles the thermal expansion of the crystal along the *b*-axis (compare Figures 10 and 4). In particular, the slight elongation of *b* below T_{23} correlates with a jump-wise increase of P_s. Also the change in slope of the $b(T)$ function correlates with different slopes of $P_s(T)$ in phases II and III. These similarities between $b(T)$ and $P_s(T)$ are justified because the *b* parameter of the unit cell is directly related to the ionic displacement δ along [010] (see Figures 8, 9, and 12), and this displacement is the main origin of P_s in dabcoHBF$_4$. The relative shifts between the cation and anion, derived from the structure determination as a function of temperature, allowed us to model the $P_s(T)$ dependence using a simple point-charge approximation. The charges were assumed to be located in the center of the ions. The calculated values of P_s are compared with experimental results in Figure 11. The excellent agreement

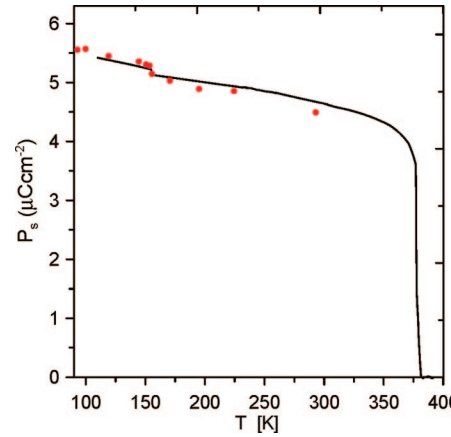

Figure 11. Temperature dependence of the spontaneous polarization in dabcoHBF$_4$ (solid line) and the P_s values calculated from the atomic displacements using the point-charge model (points).

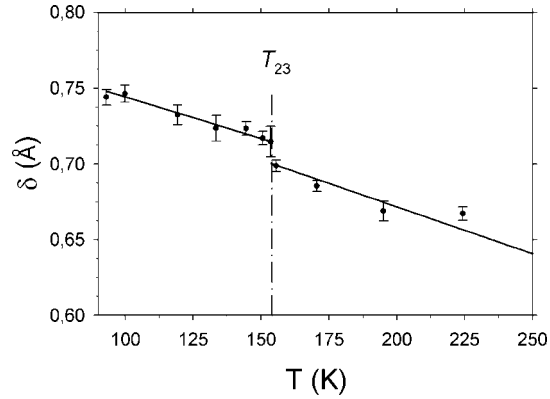

Figure 12. Temperature dependence of the ionic displacement δ through phases II an III in dabcoHBF$_4$ (cf. Figures 8 and 9) calculated from the structures determined in this study.

between the magnitudes of spontaneous polarization calculated and derived from pyroelectric measurements testifies that the contribution arising from ionic displacements is dominant for the ferroelectric properties of the crystal below and above T_{23}.

F. Dielectric Permittivity. The real part of the complex electric permittivity, measured in the vicinity of the phase transition along the ferroelectric axis, perpendicular to the NH^+···N bonds, is shown in Figure 13. This picture illustrates only the exemplary runs recorded at the measuring electric field frequency of 1 MHz, as the results obtained at frequencies from the range from 100 kHz to 10 MHz were practically identical, indicating that along the ferroelectric direction, in the vicinity of the transition temperature T_{23}, the frequency dispersion of electric permittivity is small. Only minute changes in the tangent of dielectric loss were observed at the transition temperature. As follows from Figure 13, the jump in dielectric constant at T_{23} exhibits a small, but evident hysteresis on cooling and heating the sample, testifying to the first-order character of the transition. The decrease in dielectric constant indicates that the crystal structure stiffens and its polarizability diminishes in the low-temperature phase. A similar change in ε' was observed at the transition temperature along the crystallographic direction [100], which is also perpendicular to the H-bonded chains.[8] While these results can be regarded as typical, the dielectric response of the crystal along the hydrogen bonds is very unusual: [20] at T_{23} the electric permittivity increases in a jumpwise manner and on lowering temperature it still increases reaching a maximum around 70 K (see Figure 13b). Besides the rounded dielectric anomaly is highly frequency dispersive. The anoma-

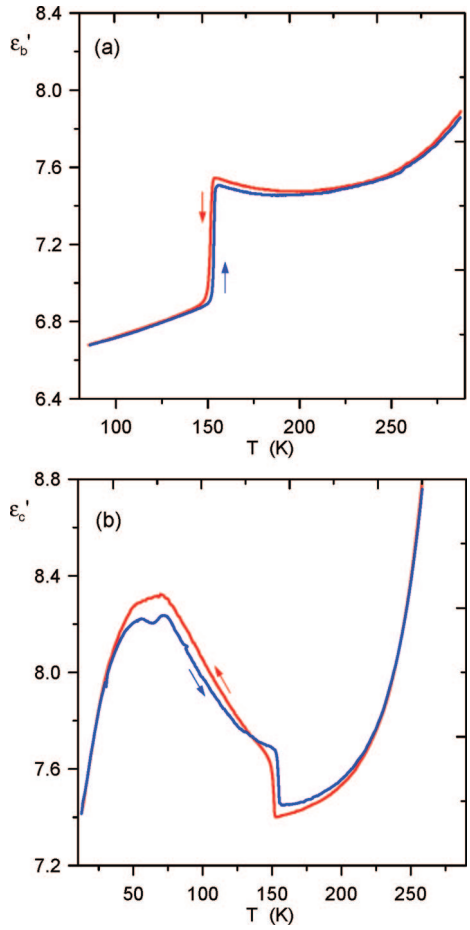

Figure 13. Dielectric constant of dabcoHBF$_4$ measured along the ferroelectric axis (a) and along the hydrogen bonded polycationic chains (b), at the electric field frequency of 1 MHz. The arrows indicate the heating and cooling runs. For more details, see ref 20.

lous dielectric response of the crystal was explained by the short-range polar regions created due to the proton transfers in the NH$^+$···N hydrogen bonds. This interpretation is consistent with the disordering of protons observed in the diffraction studies of phase III discussed in this work.

IV. Conclusions

It has been shown that low-temperature phase III of dabcoHBF$_4$ exhibits structural disorder of protons, similar to that in typical protonic glasses, where the H-atom dynamics in hydrogen bonds is responsible for specific dielectric properties.[21] For example, in the archetypal $Rb_{1-x}(NH_4)_xH_2PO_4$ (RADP)[22] and similar solid solutions, the dipolar-glass state is achieved by mixing two structurally proximate crystals with competing long-range ferroelectric and antiferroelectric interactions. This leads to a frustration effect and formation of protonic sublattice with randomly distributed protons in low temperatures. The protonic glass state develops on cooling from the high-temperature phase, where the protons are dynamically disordered in the bistable OH···O hydrogen bonds and the glassy behavior has a three-dimensional character.

The structural evidence of the H-atom disordering in the NH$^+$···N bonded ferroelectric phase III of dabcoHBF$_4$ is surprising in these respects, that dabcoHBF$_4$ is a pure substance, and that the disordering occurs on cooling from the ferroelectric phase II where the protons are ordered. Besides, because of the strictly one-dimensional character of the hydrogen-bonded network, the glassy behavior in dabcoHBF$_4$ is restricted to the direction along the hydrogen bonds. Hence the exceptional anisotropy of the dielectric response of the crystal: the relaxational dynamics existing in phase III is related to H-atom dynamics and it results in formation of short-range polar regions, essential for the relaxor-like properties of the crystal.[20] The proton dynamics in phase III is facilitated by the structural transformations removing preferences for either of the proton sites in the hydrogen bond. In particular the distances of the nitrogen atoms to the BF_4^- anions are more even in phase III than in phase II. The antiparallel arrangement of polarized H-bonded chains in dabcoHBF$_4$ phase II was contrasted with the parallel H-bonded chains in the analogous ferroelectric dabco-HReO$_4$ phase II.[2] The phase III of dabcoHBF$_4$ can be considered as their frustrated analogue, resulting from the absence of correlation between the H-sites in the neighboring chains. Owing to the linear chains building the dabcoHBF$_4$ structure, the protonic glass is truly one-dimensional, which leads to the unique anisotropy of the dielectric properties of this material.

Acknowledgment. This study was supported by the Polish Committee of Scientific Research, Grant No. 7T09A08920.

Supporting Information Available: Details of X-ray diffraction experiments and structures refinements, as well crystal data summarized in Tables S1 (phase III) and S2 (phase II) and atomic coordinates and molecular dimensions in Tables S3−S77.This material is available free of charge via the Internet at http://pubs.acs.org.

References and Notes

(1) Katrusiak, A.; Szafrański, M. *Phys. Rev. Lett.* **1999**, *82*, 576–579.
(2) Szafrański, M.; Katrusiak, A.; McIntyre, G. J. *Phys. Rev. Lett.* **2002**, *89*, 215507−1-4.
(3) Nagle, J. F.; Mille, M.; Morovitz, H. J. *J. Chem. Phys.* **1980**, *72*, 3959–3971.
(4) Jeffrey, G. A.; Saenger, W. *Hydrogen Bonding in Biological Structures*; Springer Verlag: Berlin Heidelberg, 1991.
(5) Grabowski, S. J. *Hydrogen Bonding - New Insights*; Springer: Dordrecht, 2006.
(6) Katrusiak, A. *Phys. Rev. B* **1995**, *51*, 589–592.
(7) Szafrański, M.; Katrusiak, A. *Chem. Phys. Lett.* **2000**, *318*, 427–432.
(8) Szafrański, M. *J. Phys.: Condens. Matter* **2004**, *16*, 6053–6062.
(9) Budzianowski, A. Conformational Phase Transitions in Crystals. Ph.D. thesis. Faculty of Chemistry, Adam Mickiewicz University, Poznań, 2006 (in Polish).
(10) Katrusiak, A. *J. Mol. Struct.552* **2000**, 159–164.
(11) Cugier, A. Temperature Dependence of the Crystal Structure of 1,4-diazabicyclo[2,2,2]octane perchlorate. M.Sc. thesis. Faculty of Chemistry, Adam Mickiewicz University, Ponzań, 1998.
(12) Rabold, A.; Bauer, R.; Zundel, G. *J. Phys. Chem.* **1995**, *99*, 1889–1895.
(13) Zundel, G. *Adv. Chem. Phys.* **2000**, *111*, 1–217.
(14) Katrusiak, A.; Szafrański, M. *J. Am. Chem. Soc.* **2006**, *128*, 15775–15785.
(15) Katrusiak, A. *J. Mol. Struct.* **1999**, *474*, 125–133.
(16) Sheldrick, G. M. *Acta Cryst. A* **1990**, *46*, 467–473.
(17) Sheldrick, G. M. *SHELXL97*; Program for the Refinement of Crystal Structures, University of Göttingen, Germany, 1997.
(18) Żogał, A. *Mol. Phys.* **1985**, *56*, 673–681.
(19) Katrusiak, A.; Ratajczak-Sitarz, M.; Grech, E. *J. Mol. Struct.* **1999**, *474*, 135–141.
(20) Szafrański, M.; Katrusiak, A. *J. Phys. Chem. B* **2004**, *108*, 15709–15713.
(21) Loidl, A.; Böhmer, R. In *Disorder Effects on Relaxational Processes*; Richert, R., Blumen A., Eds.; Springer-Verlag: Berlin, Heidelberg, 1994; pp 659−696.
(22) Courtens, E.; Rosenbaum, T. F.; Nagler, S. E.; Horn, P. M. *Phys. Rev. B* **1984**, *29*, 515–518.

JP801316A